ABDOMINAL SIGNALS: DIFFERENT CONCEPTS FOR RELIABLE fECG RECORDINGS

Dragos ȚARĂLUNGĂ[1], Rodica STRUNGARU[2], Mihaela UNGUREANU[3], Werner WOLF[4]

Electrocardiograma fetală (fECG) înregistrată de pe abdomenul matern are o putere mică, din cauza sursei dar şi a mediului de propagare format din diferite tipuri de țesuturi cu conductivită şi diferite. Aceste cauze duc la înregistrarea unui semnal fECG abdominal cu o amplitudine de aproximativ 10 μV. Astfel, semnalul fECG este foarte sensibil la diferite tipuri de zgomote: electrocardiograma maternă (mECG), şi interferența de la rețeaua de alimentare (PLI). Studiul prezent abordează posibilități noi de a obține un semnal fECG cu un raport semnal zgomot mult îmbunătățit. Patru concept diferite sunt definite şi analizate şi este introdusă, de asemenea, posibilitatea folosirii electrozilor concentrici pentru înregistrarea semnalului fECG.

The fetal electrocardiogram (fECG) signal recorded over the maternal abdomen has a weak power mainly due to the small source and the propagation medium formed from different types of tissue layers which have distinct conductivities. This two causes lead to an abdominal recorded fECG with an amplitude of ≈ 10 μV. Thus, abdominal fECG is very sensitive to noise interference, mainly to the maternal electrocardiogram, mECG and powerline interference (PLI). The study presents new possibilities in obtaining reliable fECG signal, i.e. with diagnostic capabilities, from abdominal recordings. Four different concepts are defined and analyzed and the concentric ring electrodes for recording fECG are introduced.

Keywords: abdominal signal, fECG signal, concentric ring electrodes, mECG signal, powerline interference

1. Introduction

Abdominal recorded signals are an alternative to cardiotocography (CTG) fetal monitoring, as they represent a method for fetal surveillance that is

[1]PhD student, Department of Applied Electronics and Information Engineering, University POLITEHNICA of Bucharest, Romania, Institut für Informationstechnik, Universität der Bundeswehr München, Germany, e-mail: dragos.taralunga@upb.ro

[2] Prof., Department of Applied Electronics and Information Engineering, University POLITEHNICA of Bucharest, Romania

[3] Prof. Department of Applied Electronics and Information Engineering, University POLITEHNICA of Bucharest, Romania

[4] Prof., Institut für Informationstechnik, Universität der Bundeswehr München, Germany

noninvasive, provides clinically significant information concerning the well being state of the fetus through the analysis of the FHR and the morphology of the fECG, and moreover, can also be used for long term monitoring. However, the fundamental problem is that abdominal signal (ADS) represents a multi-component signal containing several other disturbing components of high amplitudes besides the low amplitude fECG. Moreover, the fECG is overlapping with them in the spectral domain. Some recent publications [1], [2], [3], [4], underline that this topic currently attracts huge research efforts.

Among these perturbing bio-signals, the mECG and the PLI are clearly the main sources of disturbance. The transabdominal fECG R-peak amplitude is about 10 μV, while the amplitude of the QRS complex of the mECG shows a range for the amplitude of 0.5 to 1 mV [3].

Also, PLI is one of the most common and unwanted types of noise encountered in bio-potential measurements [5]. It is always present in biomedical recordings and a high magnitude interference can bury and degrade low voltage (power) signals like for e.g. the fECG. The source of the noise is the ac line and there are different ways in which the interference enters in the recordings: i) magnetic induction; ii) displacement currents; iii) unbalanced electrodes impedances which give rise to the "potential divider effect", i.e. common mode interference is converted into differential mode interference voltage which is amplified [6], [7].

Other disturbing signals which must be considered are the electronic noise (introduced by amplifiers etc), the slow baseline wander of signals (mainly due to electrode-skin interface), the myoelectric crosstalk from abdominal muscles and, in particular during labor, the uterine contractions. The latter evoke electrical activity which can be recorded by unipolar or bipolar electrodes placed on the abdomen of the mother, and it is usually extracted by applying a bandpass filter (0.1 – 5 Hz) to the ADS; the resulting signal is called abdominal uterine electromyogram (uEMG) or electrohysterogram (EHG), and it shows an amplitude range from 100 μV to 500 μV [8].

The large amplitudes of these noise sources are hiding the transabdominal fECG and a simple high-pass filtering of ADS for fECG extraction cannot be applied due to the over- lapping spectra of the fECG and of the noise components. Also, an application of a filter may introduce some unwanted phase distortion of the fECG. Moreover, the amplitude of the fECG depends on the electrode configuration and varies among subjects due to the different body weight and size of the mother and due to the different positions of the fetus. In addition, the recording quality of the fECG changes with time, especially with the appearance of the vernix caseosa during the last three months of pregnancy, when the R-peak of the fECG is hardly detectable [9]. Thus, it is desirable to eliminate as much

noise as possible during recording in order to apply uncomplicated software algorithms for further cleaning of the fECG signal.

The present paper describes different concepts for recording reliable fECG signal from abdominal leads, concentrating mainly on reducing the PLI and mECG interference during measurements. In this way the step for software digital processing of the ADS for the mECG, PLI removement and enhancement of the fECG signal can be eliminated, leading to simpler and faster recording systems which can be used in real time. Thus, the following different concepts are introduced:

a) high resolution ADC conversion (e.g. 22 bits) and software algorithms for PLI rejection. If the resolution of the ADC converter is small and the interference has high magnitude, then low voltage signals cannot be represented with reasonable resolution. If ADC conversion with high resolution is performed, then different types of software algorithms for removing the PLI and mECG can be applied to the recordings like: subtraction procedure [10], genetic algorithms [11], adaptive filtering [12].

b) in unipolar recordings, i.e. the common reference electrode is far from the recording electrodes, usually placed on the back [9], the PLI can be cancelled via a hardware notch filter placed at the entry of the amplification stage. Thus, the residual signals of interest from the output of the notch filter can be again amplified before sampling by ADC conversion of common resolution (16 bits);

c) in bipolar (differential) recordings using normal surface electrodes, the common mode rejection ratio of the differential amplifier is important for PLI rejection. In this paper, the unipolar abdominal signals from the electrode locations are determined by using the matrix of differential channels and a model of the inter-electrode coupling by the tissue as propagation medium, resulting in virtual quasi-monopolar recordings.

d) bipolar (differential) recordings using bipolar or recently developed tripolar concentric ring electrodes, will provide PLI rejection by placing a notch filter directly at the measuring site and also rejection of the mECG. With these types of electrodes higher sensitivity can be achieved due to the small distance between the active recording parts of the electrodes.

2. Method

2.1. The first concept for reducing the PLI and mECG from abdominal recorded signals considers the use of high resolution analog to digital, AD, conversion. The common AD converters used in ECG biomedical measurements have a resolution of 16 bits. Taking into account that the fECG recorded on the maternal abdomen has a low voltage, 10 μV [3], a resolution of 16 bits can be insufficient in a noisy environment. Thus, consider the following common

scenario where: the input range is ± 10 V, the resolution is 16 bits while the pre-amplification is 100. The voltage resolution can be computed as following:

(1)

According to (1) the desired signal has to be greater than Q in order to guarantee a change in the output code level. Ideally, if there is no presence of noise than the low voltage signal would be pre-amplified in order to be in the range of +/- 10 V, thus it is fully represented on 16 bits. But this is not the case in real situation and usually the measurements are conducted in a noisy environment where noise component has the magnitude much higher than the low voltage fECG. For this reason in general the pre-amplification is chosen in order to avoid saturation, and is typically 100. Hence, for a noise component with amplitude of 100 mV peak to peak (Vpp) and pre-amplification of 100, the number of bits to represent a fECG signal with 10 µV amplitude is .
Therefore, to ensure a good representation of the low voltage signal in digital format, an AD converter with high resolution, e.g. 24 bits, is to be used. Recently Texas Instruments produced a chip with 8 simultaneous sampled acquisition channels, 24 bits for AD conversion, built in programmable gain amplifier, internal reference and an onboard oscillator [13].

2.2. The second concept is suitable for unipolar ADS recordings. i.e. the common reference electrode is far from the active recording electrodes. Usually for unipolar recordings the power line interference has a high magnitude due to the fact that the Common Mode Rejection Ratio (CMMR) of the differential amplifiers is not exploited. Thus, this concept considers the introduction of a hardware notch filter at 50 Hz placed between the pre-amplification stage and the AD converter. Thus, new electronic boards with amplification stage and PLI reduction capabilities which are compatible with the MP 150 acquisition system from Biopac where developed. The design of the new developed electronic boards and the comparison with the amplifier used for ECG recordings, i.e. ECG100C from Biopac, are analyzed in the following paragraphs.

The layout of the boards was made with Eagle software vs. 5.9.0 Professional and the stages of the board are illustrated in Fig. 1.

Fig. 1 Typical stages for a recording channel

Each board contains the tracing for two recording channels. In total 8 boards were developed, i.e. 16 recording channels for ADS. In Fig. 2 an example of a completed board is depicted:

The notch filter stage is introduced in order to cancel the 50 Hz PLI component which distorts the abdominal fECG signal. The filter is implemented with the UAF42 universal active filter Integrated Circuit (IC) from Burr Brown. The advantage of using active filter is that they are free from switching noise and aliasing problems and are time-continuous.

In Fig. 32 the layout on the board for the notch filter stage is illustrated.

Fig. 2 Different views of the developed board

The IC of the filter can be configured as different types of low, high, band pass and notch filters. In the configuration for notch filter the output, pin 6, represents the sum of the output of a low-pass and high-pass filter both with the cutoff frequency equal with the central frequency of the notch filter.

The inputs are at pin 2 and 3 and the output is at pin 6 in Fig. 3. The notch filter stage consists of the following elements:

- In Fig. 3 resistors R_{f1} and R_{f2}, are used to set the notch frequency. For a central frequency of 50 Hz, R_{f1}=R_{f2}=3.16 MΩ:
- $$Q = 1/R * C * 2\pi, where\ R_{f1} = R_{f2} = R,\ C_1 = C_1 = C = 1000\ pF \quad (2)$$
- The bandwidth at 3 dB is controlled by changing the value of the resistor R_Q and resistor R_{Z3} in Fig. 3. The designed filter has a bandwidth at 3 dB of 3 Hz, thus R_Q = 1.54 kΩ and R_{Z3} =32.4 kΩ;
- $$R\_Q = (25\ k\Omega)\ /\ (Q - 1,)\ Q = \text{R\_z3}\ /\ (\text{R\_z1} = \text{R\_z3}\ /\ (\text{R\_z2}\ )\ ) \quad (3)$$

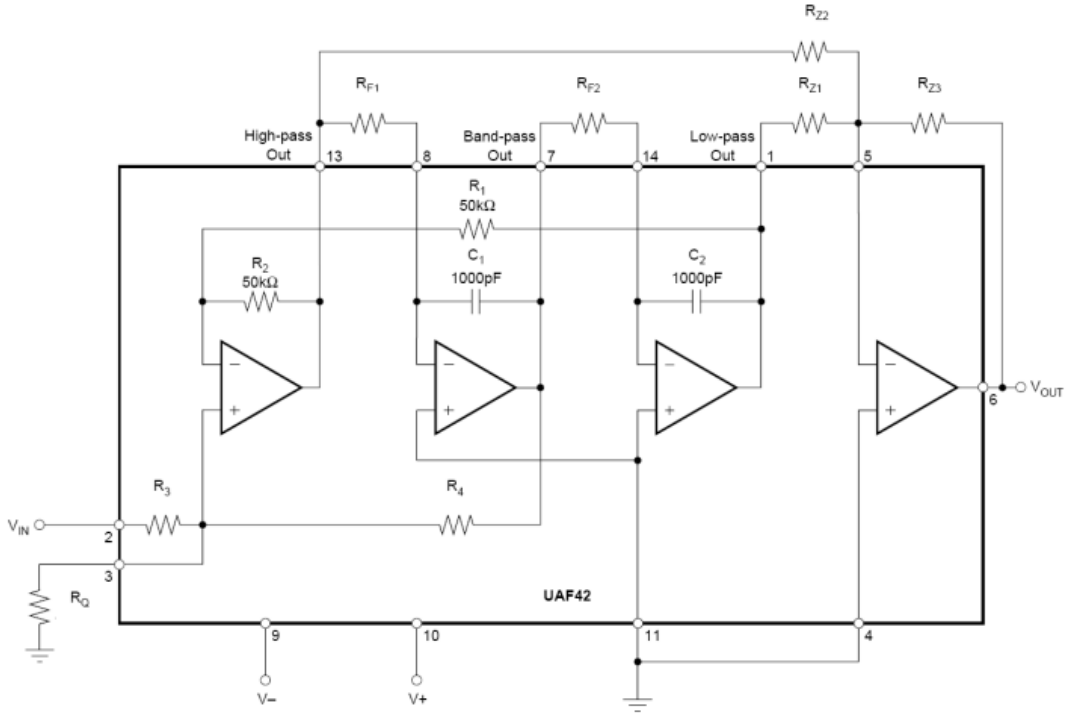

Fig. 3 Universal active filter, notch configuration [14].

2.3. The third concept for noise reduction in ADS recordings is exploiting the features of the bipolar measurements. In this case the differential amplifier rejects all common mode voltages at its input, thus an instrumentation amplifier with high common mode rejection factor (CMMR) is to be used, CMMR > 100 dB. Certainly a poor preparation of the skin produces an imbalance of the electrode - skin impedances and thus the common mode rejection capabilities of the amplifier are much reduced due to the known divider effect [5]. Nevertheless with a proper preparation of the skin and using an instrumentation amplifier with high CMMR one can obtain ADS recordings with a high signal to noise ratio, (SNR) but still corrupted with PLI. However, in this case not only the noise is cancelled but it is very probable that also the signal of interest to appear as common mode voltage between two electrodes at the input of the amplifier and thus leading to lose of information.

In the following part the possibility of deriving monopolar ADS from bipolar recordings using the matrix of differential channels and a simple model of the tissue as homogeneous propagation medium that includes the damping factor, is evaluated. Thus, initially the source of the fECG signal is modelled as a

monopolar source; the voltage measured at the surface of the abdomen is computed with the formula, [15]:

$$V_i = k * \left(\frac{1}{d_i}\right) \tag{4}$$

where d_i represents the distance from the source to the electrode placed on the maternal abdomen and $k = I_0/4\pi\sigma$ is a constant which includes the strength of the source, I_0 and the damping factor introduced by the tissue, σ. It is to be noted that quasi static conditions are considered for the volume conductor, i.e. the body tissue has just a resitive component which induces damping and no reactive component (capacitive or inductive), thus no phase shift of the signal is introduced by the propagation medium. Hence, these conditions imply that all the electric currents and fields behave, at any instant, as if they are stationary.

To begin with, the plane of electrodes on the maternal abdomen is defined in relation to the anatomical body planes: sagital, transverse and coronal (frontal) plane. Two coplanar electrodes are considered on the maternal abdomen,

Fig. 4. The maternal navel is assumed as the center of the coordinate system, represented by a black circle in

Fig. 4.

The source of the signal is represented by the green circle, S, and the electrodes by the red ones; d_1, d_2 are the distances from S to the electrode locations 1 and 2 respectively; d_{12} the distance between the two electrodes; V_1, V_2 are the unipolar potentials to be estimated and U_{12} represents the real bipolar ADS recorded with the acquisition system.

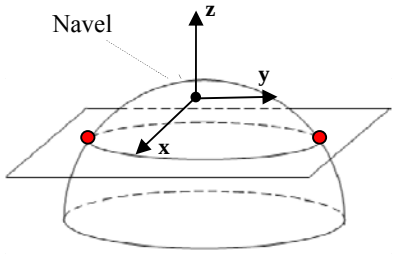

Fig. 4 Electrode plane parallel with the transverse plane and two coplanar electrodes placed on the maternal abdomen depicted here as a semi-sphere

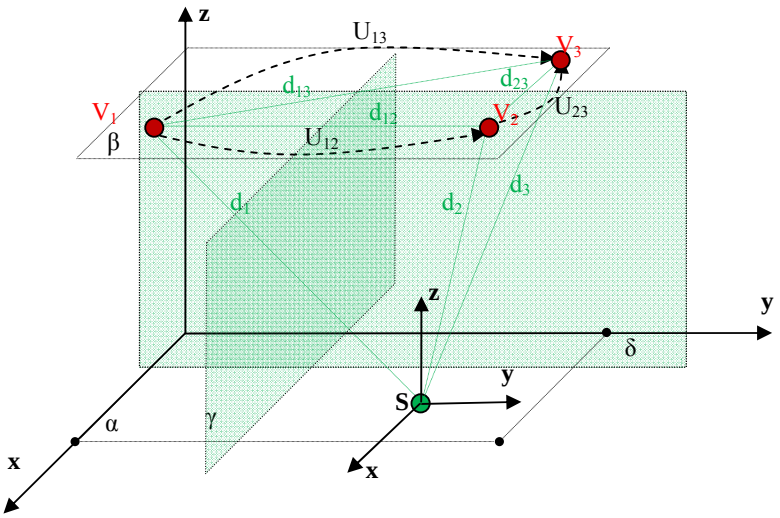

Fig. 5 Geometrical representation of the electrode and source planes when the third electrode is added

$$U_{12} = V_1 - V_2 = \frac{I_0}{4\pi\sigma}\left(\frac{1}{d_1} - \frac{1}{d_2}\right) = k\frac{d_2 - d_1}{d_2 d_1} \quad (5)$$

From (4) and (5) one can observe that the problem of estimating the unipolar measurements, V_1, V_2, reduces to a problem of source localization by determining the distances from the electrodes to the source.

The measured bipolar signal, U_{12} offers a couple of information about the position of the source. Hence the sign of the signal indicates the position of the source regarding the plane γ. The latter represents the plane perpendicular on α and β, parallel with the sagital plane and which is placed at the midpoint of the distance between the two electrodes, d_{12}. If the source is found on plane γ then $d_1 = d_2$ and $U_{12} = 0$. Hence, if $U_{12} > 0 \rightarrow d_1 < d_2$ then the source is on the "left" hand side of γ and if $U_{12} < 0 \rightarrow d_1 > d_2$ the source is on the "right" hand side. This helps to restrict the region where the source could be placed. Moreover, it should be noted that the same value of the bipolar potential, U_{12}, can be measured for different positions of the source S.

Thus two cases can be distinguished in which $U_{12} = const$ and the source has different positions in the volume conductor:

i) there are different locations of S for which $d_1 = d_2 \rightarrow U_{12} = const$. The geometrical locus of S where $d_1 = d_2$ is the intersection between two spheres: one with the centrum in electrode 1 and radius $d_1$and the second with centrum in electrode 2 and radius d_2, (6):

$$\begin{aligned}(x-x_1)^2+(y-y_1)^2+(z-z_1)^2 &= {d_1}^2\\ (x-x_2)^2+(y-y_2)^2+(z-z_2)^2 &= {d_2}^2\end{aligned} \quad (6)$$

The geometrical locus from the intersection of the two spheres is a circle, i.e. if the source is placed anywhere on this circle the bipolar measured signal is constant. The centre of the circle, C(x_c,y_c,z_c) is placed on d_{12}, and the position of it can be easily computed using equations (6) and the parametrical equations of a circle. Also the radius of the circle, r_c is obtained by applying Pythagoras theorem in the triangle formed by $d_1, d_{12}/2$ and r_c;

ii) U_{12} is a differential recording thus there can exist other pairs of (d_1, d_2), i.e. other positions of S, for which the value of $U_{12}$is constant. The pairs (d_1, d_2) can be computed from (7).

$$\frac{d_2-d_1}{d_2 d_1} = m_{12} \rightarrow d_2 = \frac{d_1}{1-m_{12}d_1} \rightarrow (d_1, d_2)\ for\ which\ U_{12} = const \quad (7)$$

Now, for each pair (d_1, d_2) the source can be located on a circle of centrum C(x_c,y_c,z_c) and radius r_c, as discussed in i). Using (7) and giving values for d_1, taking into account the restrictions $d_1 > 0, d_2 > 0$ and in this particular case $d_1 > d_2$, a discreet number of circles are obtained for which the centre and the radius can be calculated and on which the source S could be placed giving rise to $U_{12} = const$. Consequently, just one bipolar ADS recording, i.e. two electrodes, does not have sufficient information for estimating the exact position of the source S. Therefore a third electrode is added to the recording system, Fig.5.

In the case presented in Fig.5, the addition of the third electrode offers the possibility of obtaining two more bipolar recordings, U_{13} and U_{23}. The same analysis as described for U_{12} can be performed for the new bipolar recordings. Thus, if $U_{23} = V_2 - V_3 = k\frac{d_3-d_2}{d_3 d_2} > 0 \rightarrow d_2 < d_3$ then the source is on the "left" hand side of the plane δ, and if $U_{23} < 0 \rightarrow d_2 > d_3$ then the source is on the "right" hand side of the plane δ. Moreover, there are different pairs (d_2, d_3), i.e. different locations for the source, that give rise to $U_{23} = const$. As described above in the analysis for U_{12}, using the relationship between d_2 and d_3, i.e. $\frac{d_3-d_2}{d_2 d_3} = m_{23} \rightarrow d_3 = \frac{d_2}{1-m_{23}d_2} \rightarrow (d_2, d_3)$ for which $U_{23} = const$, the circles on which the source can be located in order to have $U_{23} = const$ are computed.

Now, consider that U_{12} and U_{23} are measured simultaneous, i.e. the conditions for d_1, d_2 and d_3 have to be simultaneous satisfied. Hence, triplets (d_1, d_2, d_3) for which $U_{12} = const$ and $U_{23} = const$ are generated and for each triplet (d_1, d_2, d_3) the position of the source is at the intersection between the two circles, the one obtained by the intersection of sphere 1, centrum electrode 1 and radius

d_1, with sphere 2 (center electrode 2 and radius d_2), and the circle obtained by the intersection of sphere 2 and sphere 3, (centre electrode 3 and radius d_3)**Error! Reference source not found.**.

If a forth electrode is added and the same analysis is applied for the bipolar recordings U_{23} and U_{24}, than a similar curve is obtained for the possible location of the source.

Taking into account that the source is at a specific point in space and that the three bipolar recordings are measured in the same time than the estimated position of the source is the intersection point of the two curves of the possible positions of the source, resulted from the analysis of U_{12}, U_{23} and U_{23} U_{24} respectively.

The intersection point can be determined if the analytical functions which are fitting the curves are known. Thus, the analytical function which describes the points where the source can be placed in the volume conductor is described in (8):

$$z_{est} = a + b \cdot x + c \cdot x^2 + d \cdot x^3 + e \cdot x^4 + f \cdot x^5 + g \cdot y + h \cdot y^2 + i \cdot y^3 + j \cdot y^4 + k \cdot y^5 \quad (8)$$

2.4. The fourth concept for recording reliable fECG via abdominal recorded signals consists in using newly developed bipolar and tripolar. concentric ring electrodes [16], [17]. It should be noted that this type of electrodes were not used for recording abdominal fECG until the publishing of the present manuscript thus the concept is new and brings new knowledge in the topic.

These types of electrodes are able to estimate the Laplacian of the surface potential. It was proven that Laplacian recordings have a better spatial resolution than normal bipolar recordings. Thus, consider a point P on the maternal abdomen, where the electrical potential is V_P and a local Cartesian coordinate system (x,y,z) with z axis orthogonal to on the body surface. Thus, the Laplacian can be expressed as follows:

$$L_P = \frac{\partial^2 V_P}{\partial x^2} + \frac{\partial^2 V_P}{\partial y^2} = -\frac{\partial^2 V_P}{\partial z^2} \quad (10)$$

And because of the quasi static conditions are valid the electrical field can be expressed by gradient potential, $E = -\nabla\phi$, and the current density is expressed as $J = -\sigma\nabla\phi$. By applying the divergence operator the well know Poisson equation is obtained: $\nabla J = -\sigma\nabla^2\phi$. The equation of the Laplacian can be rewritten as described in (11):

$$L_P = -\left(\frac{1}{\sigma}\right)\left(\frac{\partial J_{Px}}{\partial x} + \frac{\partial J_{Py}}{\partial y}\right) \quad (11)$$

$$L_P = \left(\frac{1}{\sigma}\right)\left(\frac{\partial J_{Pz}}{\partial z}\right) \quad (12)$$

where J_{Px} and J_{Py} are the tangential components of the current density at point P on the maternal abdomen, while J_{Pz} is the orthogonal one.

The equations (11) and (12) suggest that the Laplacian of the potential on the maternal abdomen is negatively proportional with the divergence of the tangential components of the current density on the body surface and it is proportional to the derivative of the orthogonal current component. Thus, Laplacian electrodes are able to reject the electrical activity from tangential sources (horizontal dipoles) and are more sensitive to the orthogonal sources (vertical dipoles). In other words, the electrical potentials generated by sources located far from the recording point are rejected while the potentials generated from sources positioned under the sensor are registered. In this way it provides more spatial details in differentiating multiple simultaneously active sources and source locating.

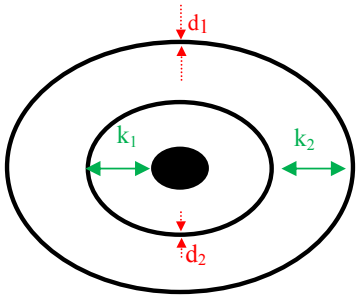

Fig. 6 the design of the concentric ring electrode

In Fig.6 a tripolar concentric ring electrode realized with an inner, middle and outer ring is depicted. d_1 and d_2 represent the width of the middle and outer ring respectively; k_1, k_2 the distance between the inner and middle ring and between the middle and outer ring respectively. The sensor can register three potentials: V_{cen}on the inner ring, V_{mid} on the middle ring and V_o on the outer ring.

In applications where very low voltage signals are registered, the quasi-bipolar configuration, i.e. when the outer ring and the inner one are in short cut, is preferred due to the fact that the recorded signal has a greater amplitude than the one recorded by the Laplacian electrode in tripolar configuration, i.e. when all rings are considered [18]. Moreover, the quasi-bipolar configuration is able to offer reliable Laplacian estimates [17], as described briefly in (13):

$$V_{out} = \frac{(V_o - V_{mid}) - (V_{mid} - V_{cen})}{2} = \frac{\Delta V_{omid} - \Delta V_{midcen}}{2} \approx \frac{d^2V}{dz^2} \quad (13)$$

The idea to use the Laplacian electrodes for improving the signal to noise ratio of the abdominal recorded fECG is based on the capability of these sensors to reject far electric fields which propagate tangential on the body surface. Hence, the mECG is generated by a source which is at a great distance from the sensor placed on the maternal abdomen surface, thus it is expected that the main disturbing component in ADS recordings, i.e. the mECG, is rejected. The first step is to design a concentric ring electrode specialized for ADS measurement which is able to record a reliable fECG and reject the mECG. However, before designing and developing the concentric ring electrodes the Laplacian potential by this type of sensor can be estimated using a special configuration of unipolar electrodes. The Laplacian in point 0 can be computed with the following equation:

$$L_0 = \frac{4}{b^2}\left(V_0 - \frac{1}{n}\sum_{i=1}^{n} V_i\right) \quad (14)$$

where V_i is the unipolar potential recorded by electrode 1, n is the number of surrounding electrodes and $b = r$ radius of the circle, [19].

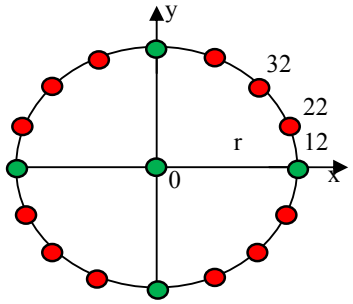

Fig. 7 Diagram of the virtual circular electrode formed with unipolar electrodes from which the Laplacian can be estimated

3. Results

3.1. In order to evaluate the performance of the new electronic boards (DEB) developed for acquiring fECG with no PLI noise a comparison is made with the ECG 100C amplifier from Biopac. The tests for the evaluation are realized using the scheme provided in Fig. 8

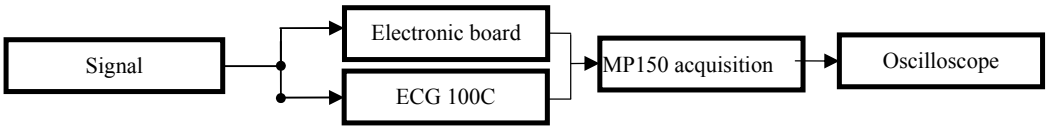

Fig. 8 Block diagram of the test configuration set up

First the bandwidth of the two acquisition amplifiers is determined. In Fig. 9 the frequency response of the DEB, of the ECG 100C and of the ECG 100C when the 35 Hz lowpass filter switch is turned on. The latter is the case when the notch filter of the ECG 100C is activated. It can be observed that the amplifier ECG100C it is not suitable for recording fECG signals because when the 35 Hz low pass filter is off, it has a bandwidth up to just 160 Hz and no power line interference suppression capability.

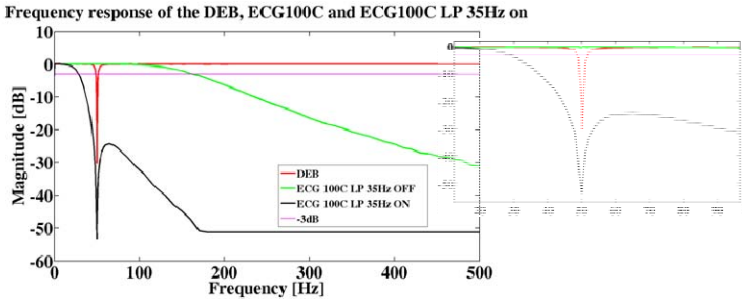

Fig. 9 Frequency response of the Deb and ECG 100C

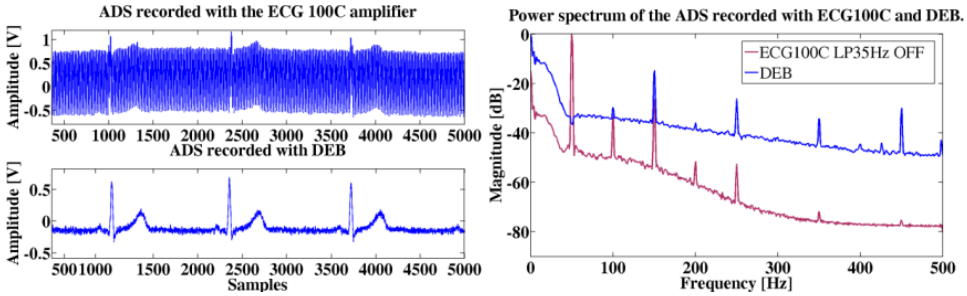

Fig. 10 a) real ADS recorded with the ECG 100C amplifier, upper subplot, and with the DEB, lower subplot; b) power spectrum of the recorded signals

When the 35 Hz low pass filter of the ECG 100C amplifier is active then also the hardware notch filter becomes active and in spite of the good attenuation, -53.2 dB, the bandwidth is too narrow, i.e. up to 29 Hz, which is not suitable even for recording ECG from adults for diagnostic purpose [20].

From

Fig. **10**a) it can be observed by visual inspection a significant improvement in cancellation of the PLI when using the DEB amplifiers. This is sustained by analysis of the estimated power spectrum in

Fig. **10**b). While the 50 Hz component has a high magnitude in the ADS recorded with the ECG 100C, it is entirely eliminated from the one recorded with the DEB amplifier.

3.2. In order to evaluate the third concept a numerical analysis is considered. In Table 1 the locations of the electrodes on the maternal abdomen and the location of the source are defined. According to the electrode locations and to equation (5), the following relations are valid: $d_2 < d_1 < d_4 < d_3 \rightarrow U_{12} < 0,\ U_{13} > 0, U_{23} > 0,$ and $U_{24} > 0$. Thus, considering the analysis described in 2.3 the possible positions of the source determined through the study of the bipolar recordings U_{12} and U_{23}, are depicted in Fig. 11 with '+' pink markers and green line.

The equation (9) represents the best analytical function that fits the possible source locations. In Fig. 11, z_{est} is represented with a green curve.

Table 1

The initial conditions of the numerical study

Coordinates	**Abdominal electrodes**				**Source location**
	1	**2**	**3**	**4**	**Fetal heart**
x	**20**	**0**	**20**	**20**	**30**
y	**20**	**20**	**20**	**40**	**15**
z	**0**	**20**	**20**	**20**	**0**

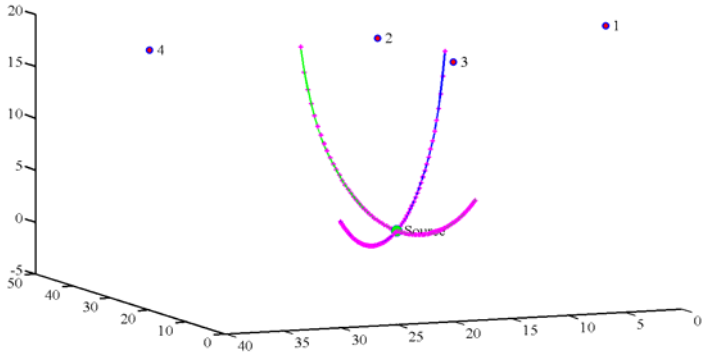

Fig. 11 Representation of the possible locations of the source determined through the analysis of the bipolar recordings U_{12}, U_{23} and $U_{23,}$ U_{24} respectively

The coefficients of the analytical function, the error and the statistical parameters of the fitting process are described in Table 2.

The same analysis is applied when considering the bipolar recordings U_{23} and U_{24}.

Table 2

Parameters of the fitting process for possible locations of the fetal heart

Coefficients	a (*10^{-7})	b(*10^{5})	c	d	e	f(*10^{-3})	g(*10^{4})	h	i	j	k
Values (U_{12} and U_{23},)	10.5	0.24	1247	-205	0.38	-1	19.8	5474	-1144	-309	26
Values (U_{23} and U_{24},)	1.04	-0.013	7596	-142	1.36	1	67.8	23579	711	-12	0.07

Table 3

Statistical parameters of the fitting process

	Values (U_{12} and U_{23},)	Values (U_{23} and U_{24},)
• Sum of the Squares due to Error (SSE): $\boldsymbol{SSE} = \sum_{i=1}^{n}(z_i - z_{est})^2$	0.13465627	0.073110735
• Sum of Squares about the mean (SSM): $\boldsymbol{SSM} = \sum_{i=1}^{n}(z_i - \bar{z})^2$	861.17755	847.65927
• Coefficient of Determination (r^2) $r^2 = 1 - \frac{SSE}{SSM}$	0.9998436615	0.9999137499
• Degree of Freedom: $\boldsymbol{df} = n - m$	74	66
• Mean Square Error (MSE): $\boldsymbol{MSE} = \frac{SSE}{df}$	0.0018196794	0.0011077384
• Root Mean Square Error (RMSE) $\boldsymbol{RMSE} = \sqrt{MSE}$	0.0426576998	0.0332827045
• Mean Square due to Regression (MSR): $\boldsymbol{MSR} = \frac{SSM-SSE}{m-1}$	86.117755	84.758616
• F-statistic: $\boldsymbol{F} = \frac{MSR}{MSE}$	47325.8	76515

where z_i are the data points, z_{est} are the estimated points using (9) , $\boldsymbol{n}$ is the data length, $\bar{z}$ is the mean of the data points,$\boldsymbol{m}$ is the number of coefficients in equation (9).

In Fig. 11 the possible positions of the source determined in this case are depicted with red "+" and the fitted curve with blue. Moreover, the points are fitted using equation (9) and the statistical parameters of the fitting process are given in Table 2.

Now, the intersection point of the two curves depicted in Fig. 11 represents the exact position of the source. It can be determined by solving the equation (15):

$$(a_1 - a_2) + (b_1 - b_2)x_s + (c_1 - c_2){x_s}^2 + (d_1 - d_2){x_s}^3 + (e_1 - e_2){x_s}^4 + (f_1 - f_2){x_s}^5 + \\ +(g_1 - g_2)y_s + (h_1 - h_2){y_2}^2 + (i_1 - i_2){y_s}^3 + (j_1 - j_2){y_s}^4 + (k_1 - k_2){y_s}^5 = 0 \quad (15)$$

The Levenberg-Marquardt algorithm is used to solve the non-linear equation described in (15). The values obtained for the locations of the source are: $\overline{x_s} = 30{,}03$, $\overline{y_s} = 14{,}98, \overline{z_s} = 0$. The error of estimation can be computed with the following :

$$\varepsilon_{x_s} = \frac{(x_s - \overline{x_s})^2}{{x_s}^2} = \ 1.0e-006, \ \ \varepsilon_{y_s} = \frac{(y_s - \overline{y_s})^2}{{y_s}^2} = \ \ 1.7778e-006 \tag{16}$$

3.3. In order to test the idea of using Laplacian electrodes in removing the mECG and enhance the fECG, the configuration in Fig. 12a) is used on a pregnant woman. The sampling frequency is 1000 Hz, the gain 5000 Hz, the bandpass 0.05 Hz – 300 Hz, and the inter-electrode distance is $b = 5\ cm$. The type of the measurement is unipolar with reference at location 11 and ground at 12.

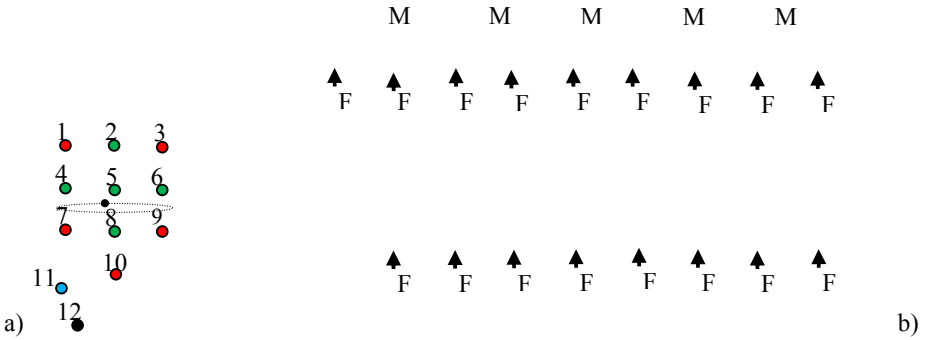

Fig. 12 a) Electrode configuration used for recording the ADS on a pregnant woman. The electrodes marked with green are used to estimate the Laplacian at location 5; b) Abdominal recorded fECG in upper plot and the estimated Laplacian at location 5 in lower one.

From Fig. 12c) it can be observed that the estimated Laplacian contains no mECG tracing while the fECG is still present.

4. Conclusions

In the present article different concepts for removing the interference introduce by the power line in order to record a fECG signal with high SNR, are discussed and analyzed.

The first concept is intuitive and basic and it considers the resolution AD conversion. A high resolution, e.g. 24 bits is needed for fECG signal recordings. In this way software algorithms can be used after the acquisition of the ADS in order to remove the power line interference and the mECG, ensuring a high

quality fECG signal. This enables the creation of medical instrumentation systems for high quality ADS recordings.

The second concept represents a hardware solution which involves the using of a notch filter. Thus, a clean ADS is obtained which can be further digitally process using different algorithms in order to eliminate also the mECG and to obtain a fECG with diagnostic capabilities which can help reduce the fetal mortality and the unnecessary chirurgical interventions.

For the third concept it can be observed that the estimation is reliable and thus the fetus heart position can be determined just by analyzing the bipolar recordings. The study can be extended to the more realistic model, i.e. considering the model of the heart to be described by a dipole. Nevertheless the same kind of analysis as the described in subsection 3.3 is required. Through this geometrical/analytical analysis the information which is likely to be canceled by the differential amplifier can be obtained, thus obtaining a more reliable fECG.

The forth concepts considers the introduction of the ring concentric electrodes for abdominal fECG recording. In literature there is no reporting of using such electrodes for obtaining the fECG, thus the analysis and results are original. The estimated Laplacian contains no mECG tracing while the fECG is still present This is an important improving for the technique of recording fECG signal via abdominal leads, because in this way the mECG, which represents the most disturbing component in these types of recordings, is eliminated during measurement thus no complex algorithm is needed to digitally process the ADS. However, the Laplacian has much smaller amplitude than the signal recorded via unipolar leads. This problem can be easily solved when using the concentric ring electrodes, which offer a more precise Laplacian than the configuration we used, by placing the pre-amplification stage at the electrode site. In this way the PLI and other common mode noise are canceled and than a much higher gain factor can be used in the final amplification stage. It should be noted that electrode 5 was not place necessarily over the fetus heart, thus higher amplitudes for the fECG signal are expected.

R E F E R E N C E S]

[1] *, K. Marsal*, ST analysis of fetal electrocardiography in labor, Seminars in Fetal and Neonatal Medicine, vol. 16, no. 1, pp. 29-35, 2011.

[2] *R. Rzepka, A. Torbé, S. Kwiatkowski, W. Blogowski, R. Czajka*, Clinical outcomes of high-risk labours monitored using fetal electrocardiography, Ann Acad Med Singapore, vol. 39, pp. 27-32, 2010.

[3] *M. Peters, J. Crowe, J. F. Piéri*, *et al,* Monitoring the fetal heart non-invasively: a review of methods, Journal of Perinatal Medicine. Vol. 29, No. 5, pp. 408–416, 2001

[4] *R. Vullings, C. H. Peters, M. J. Hermans,P. F. Wijn,S. G. Oei, J. W. Bergmans*, A robust physiology-based source separation method for QRS detection in low amplitude fetal ECG recordings, Physiol Meas. vol. 7, pp. 935-51, 2010.

[5] *J. C. Huhta and J. G. Webs*ter, 60-Hz interference in electrocardiography, IEEE Trans. Biomed. Eng., **vol.** BME – 20, No. 2, March 1973.

[6] *R. Palllas- Areny*, Interference-Rejection Characteristics of Biopotential Amplifiers: A Comparative Analysis, IEEE Trans. Biomed. Eng., **vol.** 35, No. 11, November 1988.

[7] *E. Spinelli, M. Mayosky and R. A. Pallas-Areny*, A practical approach to electrode skin impedance unbalance measurement, IEEE Trans. Biomed. Eng, **vol**. 53, pp. 1451-3, 2006.

[8] *D. Devedeux, C. Marque, S. Mansour, G. Germain, J. Duchêne* Uterine electromyography: a critical review, Am J Obstet Gynecol; vol. 169, no.6, pp. 1636-53, 1993.

[9] *A Van Oosorterom*, Lead systems for the abdominal fetal electrocardiogram, Clin. Phys. Physiol. Meas. Vol. 10, Suppl. B, 21-21, 1989.

[10] *C. Levkov, G. Mihov, R. Ivanov, et al*, Removal of power-line interference from the ECG: a review of the subtraction procedure, BioMedical Engineering OnLine, vol. 4, no. 50, 2005.

[11] *B.S.Lin, F.C. Chong*, Power-line Interference Removal of Bioelectric Signal Measurement by using Genetic Adaptive Filter, Proc. of the 2005 IEEE Engineering in Medicine and Biology 27th Annual Conference Shanghai, China, September 1-4, 2005.

[12] *B. Widrow et al.*, Adaptive noise cancelling: principles and applications, *Proc. IEEE*, vol. 63, no. 12, pp. 1692–1716, Dec. 1975.

[13] *Texas Instruments*, Low-Power, 8-Channel, 24-Bit Analog Front-End for Biopotential Measurements, available at http://focus.ti.com/docs/prod/folders/print/ads1298r.html

[14] *Burr Brown*, Precision, Low Power Instrumentation Amplifiers Datasheet, available at http://www.datasheetcatalog.com/datasheets_pdf/I/N/A/1/INA129.shtml (accessed in 2011)

[15] *J. Malmivuo, R. Plonsey*, Biolelectromagnetism, Oxford University Press, ISBN 0-19-505823-2, 1995.

[16] *W. G. Besio, K. Koka, R. Aakula, W. Dai*, Tri-polar concentric ring electrode development for laplacian electroencephalography, IEEE Trans Biomed Eng., vol. 53, no. 5, pp. 926-33, 2006.

[17] *G. Prats-Boluda, G. Casado, Y. Ye-Lin*, *et al*, Active concentric ring electrode for non-invasive detection of intestinal myoelectric signals, Med Eng Phys., vol. 33, no. 4, pp. 446-55, 2011.

[18] *M. Kaufer, L. Rasquinha, P. Tarjan,* Optimization Of Multi-ring Sensing Electrode Set**,** IEEE EMBS, Proc. of the 12th Annual International Conference of the pp.612-613, 1990.

[19] *B. He*, Theory and applications of body-surface Laplacian ECG mapping, Eng. in Med. and Biol. Mag., IEEE, vol.17, no.5, pp.102-109, 1998.

[20] P. Kligfield Recommendations for the Standardization and Interpretation of the Electrocardiogram: Part I: The Electrocardiogram and Its Technology, J Am Coll Cardiol,vol. 49, pp. 1109-1127, 2007.